Supplementary Information

Determination of Energy Level Alignment and Coupling Strength in 4,4'-Bipyridine Single-Molecule Junctions

Taekyeong Kim[1], Pierre Darancet[1,2], Jonathan R. Widawsky[1], Michele Kotiuga[2,4], Su Ying Quek[3], Jeffrey B. Neaton[2,4], and Latha Venkataraman[1]

[1]Department of Applied Physics and Applied Mathematics, Columbia University, New York, NY,

[2]Molecular Foundry, Materials Sciences Division, Lawrence Berkeley National Laboratory, Berkeley, CA,

[3]Department of Physics, Graphene Research Centre and Centre for Computational Science and Engineering, National University of Singapore, Singapore

[4]Department of Physics, University of California, Berkeley, Berkeley, CA

AUTHOR EMAIL ADDRESS: lv2117@ columbia.edu; jbneaton@lbl.gov

Contents:

1. Experimental Details:

Molecular conductance is measured by repeatedly forming and breaking gold point contacts in a solution of molecules with a custom Scanning Tunneling Microscope (STM)[1]. A freshly cut gold wire (0.25 mm diameter, 99.999% purity, Alfa Aesar) is used as the tip, and UV/ozone cleaned gold substrate (mica with 100 nm gold, 99.999% purity, Alfa Aesar) is used as the substrate. The substrate is mounted on a piezoelectric positioner (Mad City Labs), so that sub-angstrom resolution in position is achieved. During the entire break junction procedure, a small, constant bias (10 mV) is applied between the tip and the substrate with a 10kΩ series resistance added in the circuit while the current is measured (Keithley 428-Prog). Piezo control and data collection were performed using a National Instruments PXI Chassis System (with PXI-4461, PXI-6289) at 40 kHz and driven and managed with a custom-program using Igor Pro (Wavemetrics, Inc.). The experimental set-up is kept under ambient conditions. For the thermopower measurements, the substrate was mounted onto the hot side of a thermoelectric (Peltier) device, while the cold side was kept near room temperature. Additionally, the STM tip was kept near room temperature throughout the measurement. The temperature of the hot substrate and the tip was recorded using a thermocouple. The temperature limit that can be achieved in our set-up given the peltier is about 30K. For all experiments here, we carried out measurements with a temperature difference of 24K which allowed us to measure thermoelectric currents and voltages accurately. Note that since we are in a linear response regime, the thermoelectric current and voltage are linearly proportional to the temperature differences, as verified for this molecules in past work.[2, 3] In all the measurements carried out here, the entire hold section of the piezo ramp was kept under ~ 60ms due to the limits in the mechanical stability of the STM setup. Thus for individual low-G and high-G segments withint the trace, the hold time was limited to 20 ms. The distance that the piezo traveled between a low-G and high-G traces was set to 0.2 nm as this is the electrode separation between the high-G and low-G junction as found in past work.[4]

2. Additional Figures:

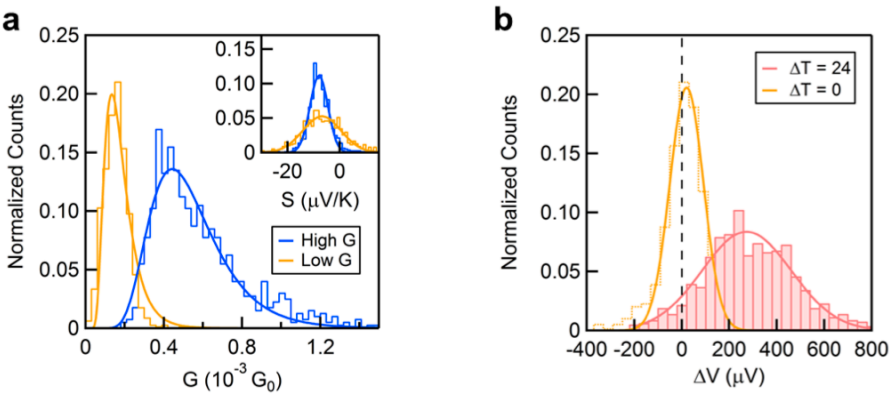

SI Figure S1: (a) Normalized histograms of conductance values determined from the slope of the IV curves of measurements with BP in the high-G (blue) and low-G (yellow) geometries. Inset: Normalized histograms of thermopower for BP junctions in the high-G (blue) and low-G (yellow) geometries. (b) Normalized histograms of ΔV for the low-G BP junction at ΔT = 24K (light red) and ΔT=0K (yellow) shown along with Gaussian fits. From the Gaussian fits we get a mean ΔV of about 250 μV at ΔT = 24 K.

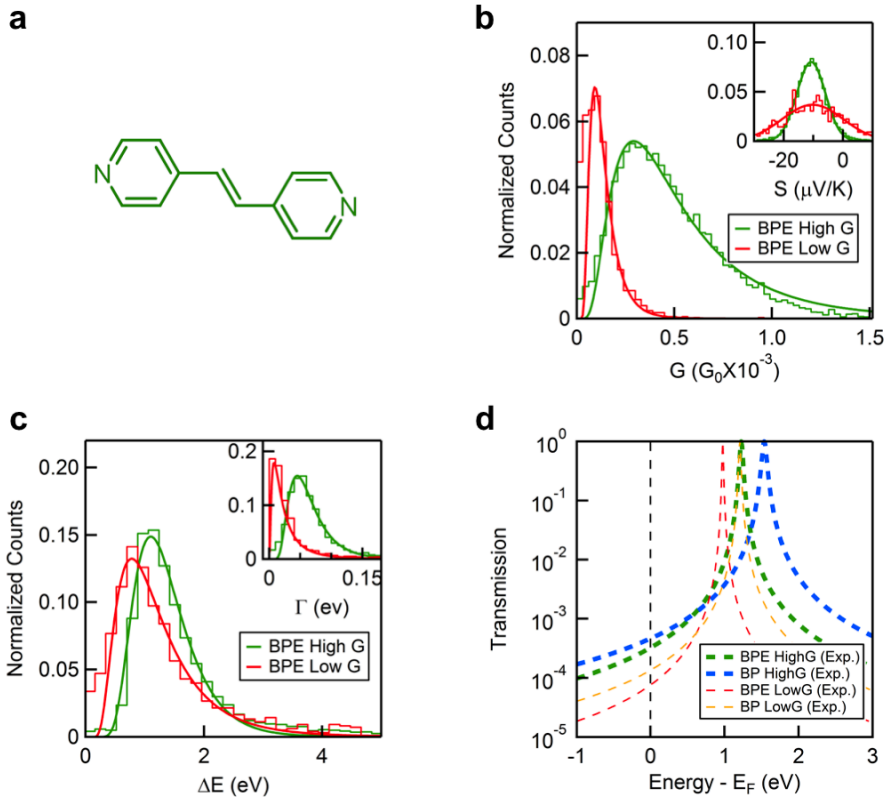

SI Figure S2: (a) Molecular structure of 1,2-di(4-pyridyl)ethylene (BPE) (b) Normalized histograms of conductance values determined from the slope of the IV curves of measurements with BPE in the high-G (green) and low-G (red) geometries. Inset: Normalized histograms of thermopower for BPE junctions in the high-G (green) and low-G (red) geometries. (c) Normalized histograms of resonance energy position relative to E_F (ΔE) for high-G (green) and low-G (red) junctions of BPE. Inset: Normalized histograms of coupling strengths (Γ) for both geometries. (d) Lorentzian curves generated using the experimental values of ΔE and Γ for BP and BPE junctions for both of high-G (thick lines) and low-G geometries (thin lines).

	ΔE_H (eV)	ΔE_L (eV)	Γ_H (eV)	Γ_L (eV)	G_H ($10^{-3}G_0$)	G_L ($10^{-3}G_0$)	S_H (μV/K)	S_L (μV/K)
BP	1.52	1.20	0.07	0.03	0.4	0.1	-8.4	-7.5
BPE	1.22	1.00	0.04	0.017	0.28	0.075	-10.1	-9.3

SI Table TS1: Resonance energy level alignment (ΔE), coupling strength (Γ), conductance (G), and thermopower (S) for high-G and low-G junctions of BP and BPE determined experimentally.

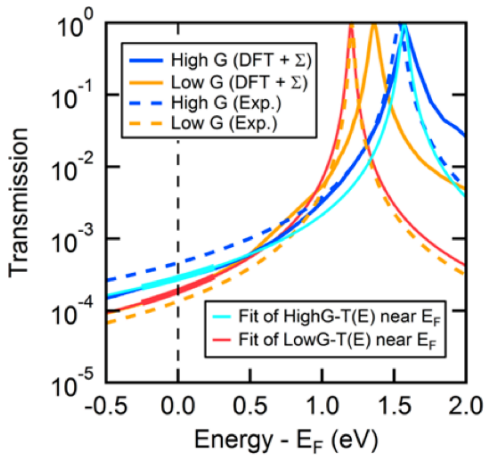

SI Figure S3: Lorentzian fits of calculated transmission functions (T(E)) near Fermi level (-250 mV to 250 mV) for high-G (light blue thick line) and low-G (red thick line) junctions of BP. The extended thin lines of the fits (thick lines) show an excellent agreement with the Lorentzian curves (dashed lines) generated using the experimental results of ΔE and Γ for both the high-G and low-G junctions.

BP	Exp.	DFT + Σ	Fit near E_F of T(E)
High-G	ΔE=1.52, Γ=0.07	ΔE=1.57	ΔE=1.57, Γ=0.055
Low-G	ΔE=1.20, Γ=0.03	ΔE=1.35	ΔE=1.20, Γ=0.033

SI Table TS2: Comparison of resonance energy level alignment (ΔE), and coupling strength (Γ) for high-G and low-G junctions between experiment and theory.

Oligophenyldiamine Series

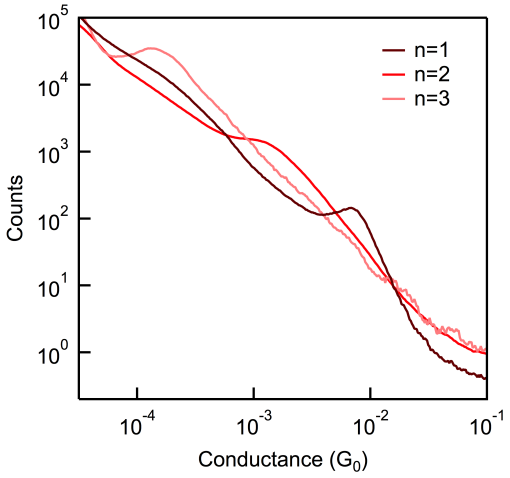

SI Figure S4: Linear binned conductance histograms for the oligophenyldiamine series analogous to measurements reported previously.[5, 6]

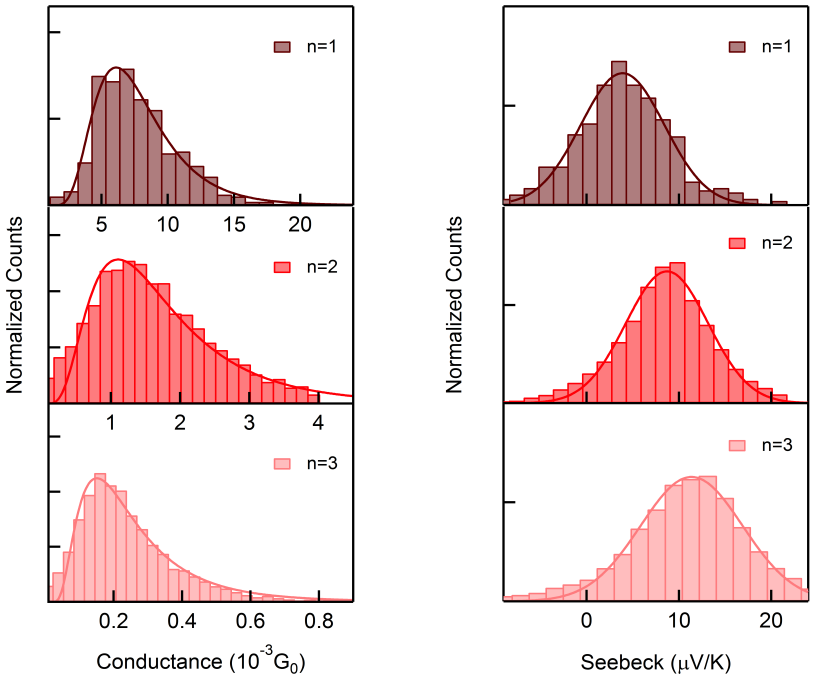

SI Figure S5: Normalized conductance and thermopower histograms of a series of oligophenyl diamine junctions. The results of the conductance from the slope of IV are consistent those measured using the scanning tunneling microscopy based break junction technique.[5, 6]

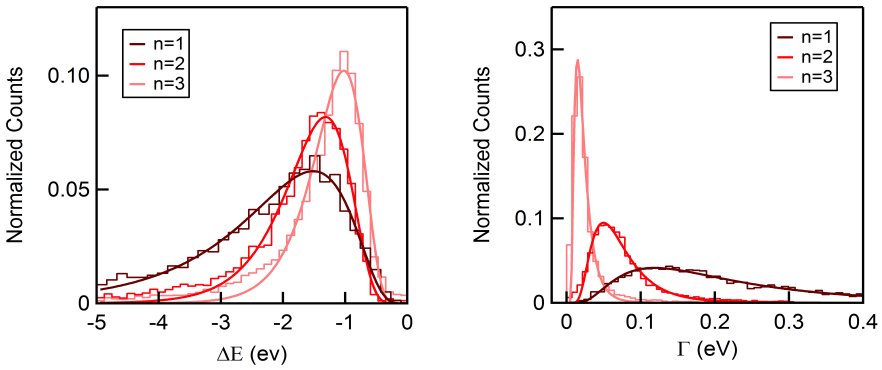

SI Figure S6: Normalized ΔE and Γ histograms of a series of oligophenyl diamine junctions.

Molecule	ΔE (eV)	Γ (eV)	G (10^{-3} G_0)	S (μV/K)
$n=1_{EXP}$	-2	0.146	6.25	3.1
$n=1_{DFT+\Sigma}$	-3.43	0.244	6.4	3.9
$n=2_{EXP}$	-1.37	0.046	1.10	7.9
$n=2_{DFT+\Sigma}$	-2.7	0.089	1.16	5.4
$n=3_{EXP}$	-1.08	0.013	0.16	10.4
$n=3_{DFT+\Sigma}$	-2.42	0.031	0.18	8.1

SI Table TS3: Resonance energy level alignment (ΔE), coupling strength (Γ), molecular conductance (G) and thermopower (S) for a series of oligophenyl diamines determined experimentally and theoretically.

Results from an alternate piezo modulation scheme:

We used a slightly different piezo ramp to carry out measurements analogous to those described in the manuscript. The ramp is illustrated in the top panel of Figure S6a and includes a pull of 2.5 nm then a hold section that lasts 20 ms, followed by a second pull of 0.2 nm followed by a second hold of 20 ms before a final pull of 2.5 nm. During each hold portion, an IV curve is measured using a voltage range of ±5 mV. The conductance and thermopower are determined and used to extract the ΔE and Γ for BP junctions that switch from a high-G configuration to a low-G configuration. The results from these measurements are consistent with those presented in the manuscript.

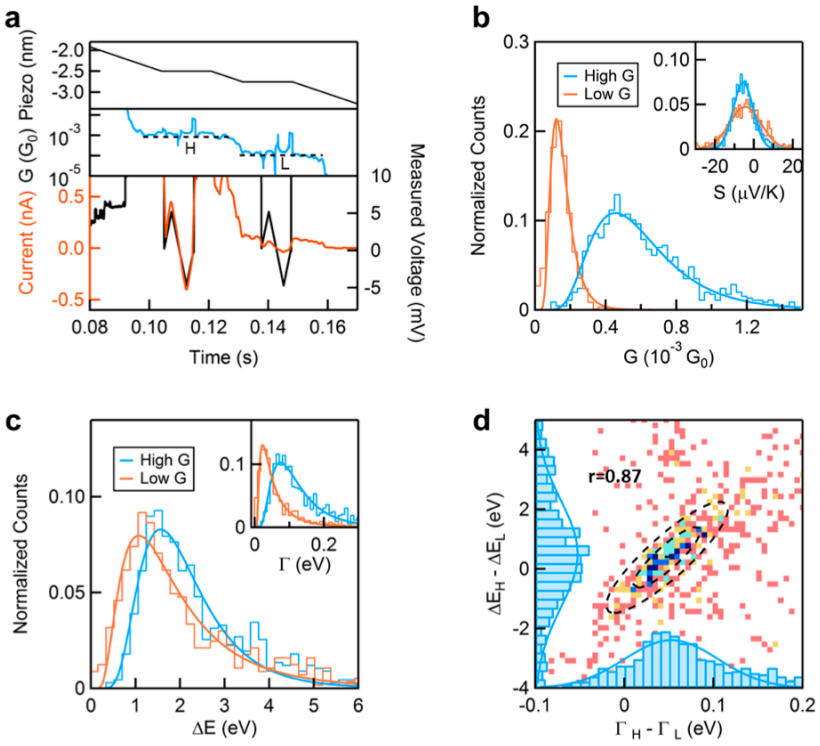

SI Figure S7: (a) Single sample trace of a BP high-G junction that is elongated to yield a low-G junction. The upper panel shows the piezo ramp, the middle panel shows the conductance and the lower panel shows the measured current (left axis) and voltage (right axis). (b) Normalized histograms of conductance values determined from the slope of the IV curves of measurements with BP in the high-G (light blue) and low-G (orange) geometries. Inset: Normalized histograms of thermopower for BP junctions in the high-G (light blue) and low-G (orange) geometries. (c) Normalized histograms of resonance energy position relative to E_F (ΔE) for high-G (light blue) and low-G (orange) junctions of BP. The inset shows normalized histograms of coupling strengths (Γ) for each geometry. (d) Correlation plot for the change in the resonance position (ΔE_H - ΔE_L) and the change in coupling (Γ_H - Γ_L) from a high-G to a low-G junction in every trace. The cross-correlation parameter r is 0.87. The peaks from the histogram of the changes are 0.35eV for (ΔE_H - ΔE_L) and 0.045 eV for (Γ_H - Γ_L).

3. Cross-correlation Analysis:

Figure S7 shows the joint probability distribution of the change in the resonance position (ΔE_H - ΔE_L) and the change in coupling (Γ_H - Γ_L) from a high-G to a low-G junction. Considering the individual variables to be normally distributed, we can model the joint distribution by a generalized two-dimensional normal distribution[7]:

$$z = A\, exp\left[\left(\frac{-1}{2(1-r^2)}\right)\left(\left(\frac{x-\mu_x}{\sigma_x}\right)^2 + \left(\frac{y-\mu_y}{\sigma_y}\right)^2 - \left(\frac{2r(x-\mu_x)(y-\mu_y)}{\sigma_x\sigma_y}\right)\right)\right] \quad \text{with} \quad r \in [-1, +1]$$

where A is the scaling parameter, r is the cross-correlation, and μ and σ are the mean value and standard deviation, respectively.

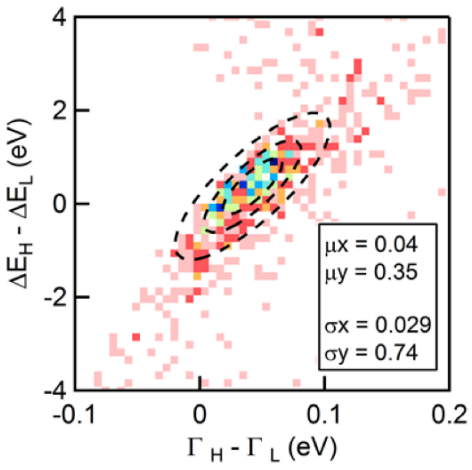

SI Figure S8: Plot of the change in resonance position (ΔE_H -ΔE_L) and the change in coupling (Γ_H - Γ_L) from a high-G to a low-G junction. The mean value of (ΔE_H -ΔE_L) is 0.35 eV (μ_y) and the mean value of (Γ_H - Γ_L) is 0.04 eV (μ_x) from the plot.

4. Theoretical Calculation Details:

First-Principles Optimization of Junction Geometries

We use DFT and the SIESTA package to obtain the self-consistent density with localized numerical orbitals and a 300 Ry grid cutoff, a 0.05 eV electronic smearing, on a 4×4 k-point sampling in directions perpendicular to the junction. Hellmann-Feynman forces on the atoms are reduced to 0.04 eV/Å or less using a GGA-PBE functional using double-ξ-basis set. We model our system consists of 7-layers of 16 gold atoms (a 4×4 unit cell) on both sides, the last 4 layers being constrained to the bulk (PBE) geometry.

Procedures for Transmission and Thermopower Calculations

The transmission function is calculated using an energy grid of 100 points between E_F - 5eV and E_F + 5eV, with 100 supplementary points between E_F - 50meV and E_F + 50meV on a 16x16 $k_{||}$ sampling in the directions perpendicular to the junctions, using the Scarlet code. We correct the Kohn–Sham excitation energies with a one-shot model DFT +Σ method. Specifically, we correct the gas-phase gap with a ΔSCF calculation, and correct for the lack of static nonlocal correlation effects through an electrostatic "image charge" model. G and S are then determined from the transmission and its derivative at E_F. Numerical evaluation of the derivative of T(E) generally requires a very fine $k_{||}$-point sampling. To minimize sampling errors, we fit T(E) around E_F with a smooth polynomial function, and take its derivative analytically.

5. References:

1. Kamenetska, M.; Koentopp, M.; Whalley, A. C.; Park, Y. S.; Steigerwald, M. L.; Nuckolls, C.; Hybertsen, M. S.; Venkataraman, L. *Physical Review Letters,* **2009,** 102, (12).
2. Malen, J. A.; Doak, P.; Baheti, K.; Tilley, T. D.; Segalman, R. A.; Majumdar, A. *Nano Lett.,* **2009,** 9, (3), 1164-1169.
3. Widawsky, J. R.; Darancet, P.; Neaton, J. B.; Venkataraman, L. *Nano Lett.,* **2012,** 12, (1), 354-358.
4. Quek, S. Y.; Kamenetska, M.; Steigerwald, M. L.; Choi, H. J.; Louie, S. G.; Hybertsen, M. S.; Neaton, J. B.; Venkataraman, L. *Nat. Nano.,* **2009,** 4, (4), 230-234.
5. Venkataraman, L.; Klare, J. E.; Nuckolls, C.; Hybertsen, M. S.; Steigerwald, M. L. *Nature,* **2006,** 442, (7105), 904-907.
6. Kim, T.; Vázquez, H.; Hybertsen, M. S.; Venkataraman, L. *Nano Lett.,* **2013,** 13, (7), 3358-3364.
7. Cramer, H., *Mathematical methods of statistics*. Princeton University Press: New Jersey, USA, 1946.